Chemical Science

ROYAL SOCIETY OF CHEMISTRY

EDGE ARTICLE

View Article Online
View Journal | View Issue

Cite this: *Chem. Sci.*, 2022, **13**, 9973

All publication charges for this article have been paid for by the Royal Society of Chemistry

Received 28th April 2022
Accepted 31st July 2022

DOI: 10.1039/d2sc02381d

rsc.li/chemical-science

Reliably obtaining white light from layered halide perovskites at room temperature†

Ethan J. Crace,[a] Alexander C. Su [a] and Hemamala I. Karunadasa *[ab]

The recent observation of broadband white-light emission from the inorganic sheets of certain layered lead-bromide perovskites has instigated a multitude of studies on this unusual phenomenon. However, the vast majority of layered bromide perovskites have flat (001) inorganic sheets and display a narrow photoluminescence at room temperature. A handful of heavily distorted (001) perovskites display broad emission, but to date, there is no method of predicting which perovskites will produce white light at room temperature prior to screening different organic molecules that can template 2D perovskites and crystallizing and analyzing the material. By studying ten Pb–Cl perovskites, we find that they all exhibit a broad yellow emission, which is strikingly invariant despite different distortions in the inorganic framework seen across the series. We postulate that this broad emission is intrinsic to all layered Pb–Cl perovskites. Although broad, the emission is not white. By adding Br to the Pb–Cl perovskites we obtain both the narrow emission and the broad emission such that the combined emission color smoothly varies from yellow to warm white to cold white as a function of the halide ratio. Thus, alloying Br to Pb–Cl perovskites appears to be a simple and general strategy for reliably obtaining white light at room temperature from (001) perovskites, regardless of the templating effects of the organic molecules, which should greatly expand the number of white-light-emitting layered perovskites.

1. Introduction

The photoluminescence (PL) of two-dimensional (2D) halide perovskites has been studied for decades, revealing emission energies that range from the infrared to the ultraviolet.[1] More recently, in 2014, a broadband emission that covered the entire visible spectrum was reported to originate from the inorganic sheets in 2D Pb–Br [2] and Pb–Cl [2b] perovskites at room temperature. To date, more than a dozen room-temperature white-light-emitting 2D perovskites[2,3] and several related low-dimensional metal-halides[3a,4] have been reported, with numerous studies converging on exciton self-trapping as the operative emission mechanism.[2b,3a,h,4b,c,5] Here, tightly bound excitons (photogenerated electron–hole pairs) create transient deformations in the inorganic framework through strong exciton-phonon coupling.[6] Radiative decay of such self-trapped excitons (STEs) affords broad PL with a large Stokes shift. Both static excited-state lattice distortions[5,7] and dynamic lattice rearrangements in the vicinity of the STE[8] have been invoked to explain the photophysics of the broadband white emission. Furthermore, numerous studies have sought to articulate relationships between the perovskite crystal structure and the energy and width of the broad emission, implicating both inter- and intra-octahedral distortions of the lead-halide octahedra. However, these subtle distortions in the inorganic lattice, often templated by hydrogen bonding interactions with the organoammonium groups, are extremely difficult to predict prior to crystallization and absolute structure determination of the perovskite. Even slight modification of the cation can lead to a very different perovskite structure or a non-perovskite phase.[2] Thus, the isolation and identification of new white-light-emitting perovskites remains serendipitous.

Herein, we study a series of ten layered Pb–Cl perovskites (Fig. 1) and find a strikingly similar broad PL, where the emission energy and width is independent of distortions in the inorganic framework. We outline a simple strategy for tuning this emission to produce white light at room temperature from 2D perovskites, without requiring specific templating interactions from the organic cations.

[a]*Department of Chemistry, Stanford University, Stanford, California 94305, USA. E-mail: hemamala@stanford.edu*

[b]*Stanford Institute for Materials and Energy Sciences, SLAC National Accelerator Laboratory, Menlo Park, California 94025, USA*

† Electronic supplementary information (ESI) available: Experimental details, definition and calculation of intraoctahedral and interoctahedral distortion parameters, crystallographic data, and spectra are in the ESI.† The CIFs for (BIEA)$PbBr_4$ at 100 K, (BIEA)$PbBr_4$ at 300 K, (BIEA)$PbCl_4$ at 100 K, (BIEA)$PbCl_4$ at 300 K, (IEA)$PbCl_4$ at 100 K, (IEA)$PbCl_4$ at 300 K, (IMA)$PbCl_4$ at 100 K, (IMA)$PbCl_4$ at 300 K, have been deposited in the CCDC under deposition numbers 2169138–5, respectively. CCDC 2169138–2169145. For ESI and crystallographic data in CIF or other electronic format see **https://doi.org/10.1039/d2sc02381d**

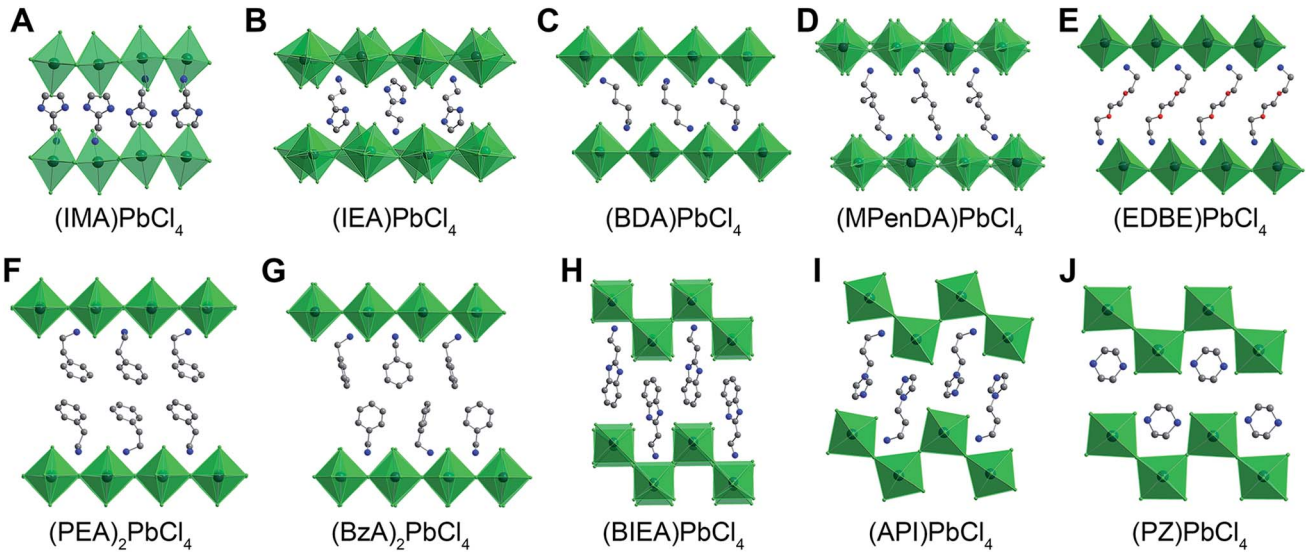

Fig. 1 Crystal structures of Pb–Cl perovskites containing (A) 2-(ammoniomethyl)-1*H*-imidazol-3-ium (IMA), (B) 2-(2-ammonioethyl)-1*H*-imidazol-3-ium (IEA), (C) butanediammonium (BDA), (D) 2-methyl-1,5-pentanediammonium (MPenDA), (E) 2,2′-(ethylenedioxy)bis(ethylammonium) (EDBE), (F) phenethylammonium (PEA), (G) benzylammonium (BzA), (H) 2-(2-ammonioethyl)-1*H*-benzimidazol-3-ium (BIEA), (I) 1-(3-ammoniopropyl)imidazolium (API), and (J) piperazinium (PZ) cations. A through G show (001) perovskites and H through J show (110) perovskites. Pb–Cl octahedra are shaded in green, red, blue, and gray spheres denote O, N and C atoms, respectively. Hydrogen and disordered atoms are omitted for clarity.

2. Results and discussion

2.1. Photoluminescence from layered Pb–Br perovskites

Upon UV or near-UV excitation, the vast majority of 2D Pb–Br perovskites exhibit narrow PL with a small Stokes shift at room temperature, attributed to the radiative decay of free excitons (FEs).[9] These (001) perovskites have flat inorganic sheets that correspond to slices cut along the (001) crystallographic plane of the three-dimensional (3D) parent perovskite. The rarer (110) perovskites feature corrugated inorganic sheets corresponding to slices cut along the (110) crystallographic plane of the 3D perovskite. Intriguingly, all (110) Pb–Br perovskites discovered to date show broadband emission at room temperature, centered at 2.1–2.4 eV with a full width at half maximum (fwhm) of 0.7–1.0 eV.[2,3a,c,d,4a,b,10] Unfortunately, (110) perovskites remain rare and difficult to predictably crystallize. Thus, reliably obtaining white light from the ubiquitous (001) perovskites, especially at room temperature, is highly desirable.

2.2. Photoluminescence from layered Pb–Cl perovskites

The PL of Pb–Cl perovskites has received much less attention than that of the bromides, although one of the earliest examples of white-light emission was seen in the (001) perovskite (EDBE)$PbCl_4$.[2b] Recently, at least six more Pb–Cl perovskites have been found to emit warm white PL.[3b,e–i] To understand the generality of the broad PL in Pb–Cl perovskites, we synthesized ten different examples featuring both (001) (Fig. 1A–G) and (110) sheets (Fig. 1H–J) and varying distortions of the inorganic framework. The optical properties of this diverse subset of perovskites allow us to propose that room-temperature broad emission is common to all 2D Pb–Cl perovskites. Notably, the emission energy and width appear unaffected by distortions in the inorganic framework.

The Cambridge Structural Database contains 27 examples of (001) Pb–Cl perovskites,[2b,3e,11] and three examples of the rarer (110) Pb–Cl perovskites.[3b,c,12] Many of these original reports only describe the crystal structure, with no optical data. We synthesized five known (001) perovskites containing butanediammonium (BDA), 2-methyl-1,5-pentanediammonium (MPenDA), 2,2′-(ethylenedioxy)bis-(ethylammonium) (EDBE), phenethylammonium (PEA), and benzylammonium (BzA) organic cations and two known (110) perovskites with 1-(3-ammoniopropyl)imidazolium (API) and piperazinium (PZ) cations. In addition to these seven perovskites, we synthesized novel perovskites with 2-(ammoniomethyl)-1*H*-imidazol-3-ium (IMA), 2-(2-ammonioethyl)-1*H*-imidazol-3-ium (IEA), and 2-(2-ammonioethyl)-1*H*-benzimidazol-3-ium (BIEA) cations. These perovskites were chosen because they exhibit a wide range of intra- and inter-octahedral distortions in the inorganic sheets (Tables 1 and S5–6†).

All ten perovskites showed strikingly similar optical properties at room temperature, despite the marked differences in their crystal structures (Fig. 2). Thin-film transmission measurements reveal that the ten Pb–Cl perovskites exhibit an excitonic absorption feature at an average energy (and standard deviation) of 3.79(9) eV. Upon UV excitation, we observe only a broad emission (BE) from these materials, which we attribute to STEs (Fig. 2 and S1–10†) in analogy to their Pb–Br congeners.[3j] Across all these perovskites, the BE peaks at 2.06(9) eV with a fwhm of 0.84(7) eV (Fig. S1–10, Tables 1 and S5–S6†) with the PL appearing yellow or warm white. The emission that appears closest to sunlight occurs in (EDBE)$PbCl_4$, with CIE chromaticity

Table 1 Intra- and inter-octahedral distortion parameters and the broad emission (BE) of the 10 Pb–Cl perovskites. See ESI for structural analyses and graphical representations

Cation	Δ_{oct} ($\times 10^{-4}$)	σ^2_{oct}	D_{out} (°)	Stokes shift (eV)	Emission maximum (eV)	fwhm (eV)
IMA	0.213	13.94	2.69	1.78	2.11	0.82
IEA	28.4	109.6	16.7	1.92	2.00	0.76
BDA	1.95	28.85	1.72	1.59	2.15	0.91
MPenDA	0.738	5.167	19.4	1.78	2.08	0.94
EDBE	0.558	800.8	16.9	1.58	2.20	0.91
PEA	8.31	18.17	6.42	1.66	2.05	0.87
BzA	0.411	22.10	0.00	1.67	2.13	0.90
BIEA	27.9	79.61	—	1.86	1.96	0.89
API	15.4	16.73	—	1.76	1.93	0.77
PZ	2.10	32.23	—	1.64	2.01	0.75

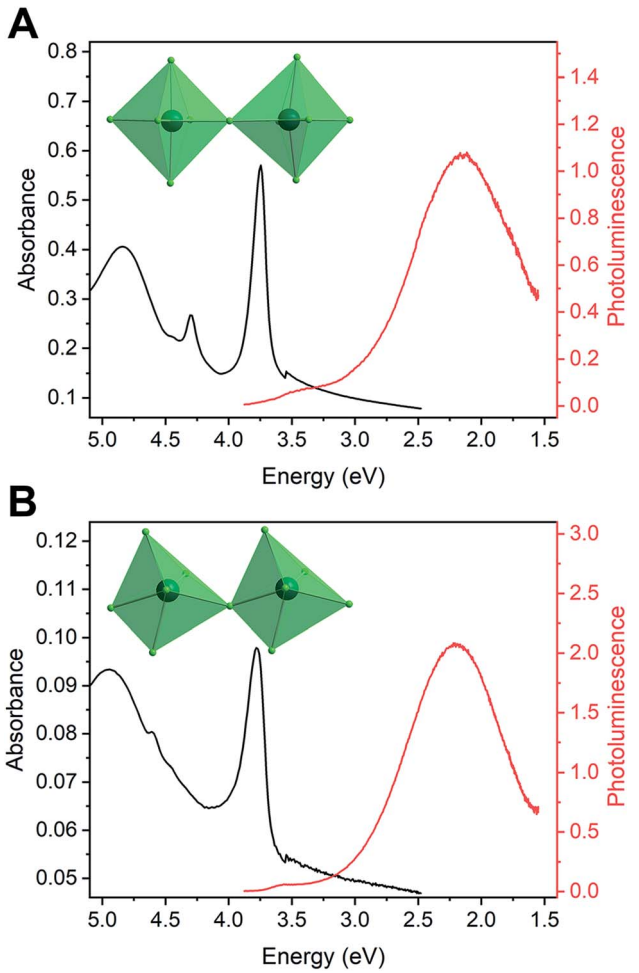

Fig. 2 Thin-film absorbance (black) and photoluminescence intensity (red) of (A) (BDA)$PbCl_4$ and (B) (EDBE)$PbCl_4$ with insets showing Pb–Cl octahedra. The step at 3.54 eV in the absorbance spectra is due to a change in the instrument light source.

coordinates of (0.32, 0.39), a color rendering index (CRI) of 80, and a correlated color temperature (CCT) of 6073 K (Fig. S11 and Table S4†). For comparison, noon-day sunlight (based on the D65 standard illuminant) has chromaticity coordinates of (0.31, 0.33) and CCT of 6504 K.[13] PL from the other perovskites appeared warmer in color, reaching a minimum CCT of 3543 K for (API)$PbCl_4$ (Fig. S11 and Table S4†).

The strong similarity in the PL of the Pb–Cl perovskites is striking given the variation in their crystal structures. A number of different structural parameters have been proposed as metrics to predict or explain the BE in Pb–Br perovskites. The most prominent is intraoctahedral distortion, which is usually measured with the parameters Δ_{oct},[14] σ^2_{oct},[15] and λ_{oct}[15] that represent the deviation in average Pb–Br bond length, the cis Br–Pb–Br bond angle, and the deviation of Pb–Br bond length in an octahedron from that predicted by an ideal octahedron of the same volume, respectively. See the ESI† for complete definitions of these parameters. Various reports[3a,c,f,h,j,16] correlate the width of the BE in 2D lead-halide perovskites and other lead-halides to these octahedral distortion parameters. Specifically, perovskites with larger degrees of octahedral distortion are expected to have broader PL. (Note that the spectra must be converted to energy units using the Jacobian transformation prior to analyzing the optical data due to the width of the emission. Spectra shown in nm in some prior reports cannot be fit correctly.)[17] We see no correlation between octahedral distortion parameters and the BE width in the ten Pb–Cl perovskites under study (Fig. 2, S12–15†). For example, (EDBE)$PbCl_4$ is the most distorted perovskite in this data set by a wide margin when considering σ^2_{oct} and the emission has a fwhm of 0.91 eV. In contrast, (BDA)$PbCl_4$ is one of the least distorted perovskites in the data set, based on all distortion parameters, and yet it too has a fwhm of 0.91 eV.

We then considered interoctahedral distortions. For example, the out-of-plane tilt of the Pb–Br octahedra ($D_{out} = 180° - \theta_{out}$ where θ_{out} is the out-of-plane component of the Pb–Br–Pb angle and the plane is defined by three adjacent lead atoms in the inorganic sheet)[3j] was previously shown to be correlated with the propensity to favor the BE from STEs over the narrow emission (NE) from free excitons (FEs) in (001) Pb–Br perovskites. The perovskites (IMA)$PbCl_4$ and (IEA)$PbCl_4$ both contain similar cations with differences only in the length of the alkyl chain. However, the inorganic sheets are quite different; (IMA)$PbCl_4$ has a small D_{out} value of 2.69° whereas (IEA)$PbCl_4$ has one of the largest D_{out} values in this data set at 16.7° (Table

1). Despite this large variation in D_{out}, the Stokes shift, E_{max}, and fwhm differ by only 140, 110, and 60 meV, respectively. Further, no general trends appear when all ten perovskites are examined (Fig. S22†). For example, (IEA)$PbCl_4$ and (EDBE)$PbCl_4$ have very similar values for D_{out}, (16.7° and 16.9°, respectively) but the differences in their emission energy and width are larger than those between (IMA)$PbCl_4$ and (IEA)$PbCl_4$.

Expanding our search to other intra-octahedral (*e.g.*, Δ_{oct}, λ_{oct}) and inter-octahedral parameters (*e.g.*, Pb–Pb distance, Cl–Cl distance) (Tables S5–6†) also yields no correlations with the BE of the (001) Pb–Cl perovskites (Fig. S12–22†). Including the (110) perovskites into our analysis further suggests that these distortion parameters do not appear to predict the PL energy or width of the 2D Pb–Cl perovskites (Fig. S12–21†).

2.3. Photoluminescence from layered Pb–Cl/Br perovskites

2.3.1 Halide composition and the broad emission (BE). Based on our studies of ten perovskites, we postulate that room-temperature BE is common to all Pb–Cl layered perovskites. However, this emission does not appear white because it lacks blue light. The typically blue NE dominates the PL of most (001) Pb–Br perovskites. We therefore hypothesized that mixed Pb–Cl/Br perovskites should reliably yield white light at room temperature at some critical halide ratio. Halide mixing has been used to change the CCT and improve the color rendition of white-light-emitting Pb–Br perovskites. For example, (*N*-MEDA)$PbBr_4$ has a CRI of 82 and emits warm white light whereas (*N*-MEDA)$PbCl_{0.5}Br_{3.5}$ has a CRI of 85 and emits cold white light.[2a] To our knowledge, however, mixed chloride-bromide perovskites have not been previously proposed as a composition that will always yield white light.

We examined the $(PEA)_2PbCl_{4-x}Br_x$ (Fig. 3A and Table S7†) perovskites where the $x = 0$ and 4 endmembers crystallize in the same space group with similar lattice parameters and structures. Thus, any changes in optical properties in this series can be attributed to the halide composition without being confounded by simultaneous structural changes. The halide ratios were determined through elemental analysis of the crystalline products to obtain more accurate values instead of using the ratio of precursors in solution during crystallization. For $x <$ 1.19 (Cl rich), only the BE is evident. As the bromide content increases from $x = 1.19$ to 3.13, the BE decreases in intensity relative to the NE (Fig. 3A) and the ratio ln(BE/NE) decreases approximately linearly with increasing x (Fig. 3B). We can use this linear relationship between ln(BE/NE) and x to fine-tune the compositions that emit white light at room temperature. The composition we synthesized that most closely matches noon day sun is $(PEA)_2PbCl_{2.81}Br_{1.19}$, with chromaticity coordinates of (0.34, 0.39), a CCT of 5228 K, a CRI of 86, and a photoluminescence quantum yield (PLQE) of 2% (Table S7†).

In addition to the changes in ln(BE/NE), the halide ratio changes the positions of the NE and BE. As expected, the PL excitation spectra show an excitonic peak that displays a 290 meV redshift from 3.32 eV to 3.03 eV as bromide content increases from $x = 1.19$ to 3.13 (Fig. S24†). The bandgaps of halide perovskites decrease as the electronegativity of the halide decreases and the excitonic absorbance is expected to follow the same trend as the bandgap.[1] The NE accordingly redshifts from 3.14 eV to 2.99 eV across this same composition range. As the excitonic absorption and NE redshifts with increasing x, the Stokes shift for the NE decreases from 180 meV to 40 meV. Interestingly, the BE behaves differently, with a linear blueshift from 2.08 eV to 2.48 eV with increasing Br content (Fig. 3A and S25†). A similar blueshift of the broad emission was observed in $(MPenDA)PbCl_{4-x}Br_x$, where the CCT of the white emission was tuned with halide mixing.[3h] The blueshift of the BE coupled with the redshift of the excitonic absorption in $(PEA)_2PbCl_{4-x}Br_x$ causes a decrease in Stokes shift from 1.24 eV to 0.55 eV with increasing x.

We then synthesized the mixed-halide series $(BDA)PbCl_{4-x}Br_x$ and $(IEA)PbCl_{4-x}Br_x$ to determine if other (001) perovskites could be tuned to emit white light at room temperature. For $(BDA)PbCl_{4-x}Br_x$, the evolution of the PL with the addition of bromide is similar to what we observed in $(PEA)_2PbCl_{4-x}Br_x$ (Fig. S26†). Increasing x results in a gradual reduction in intensity

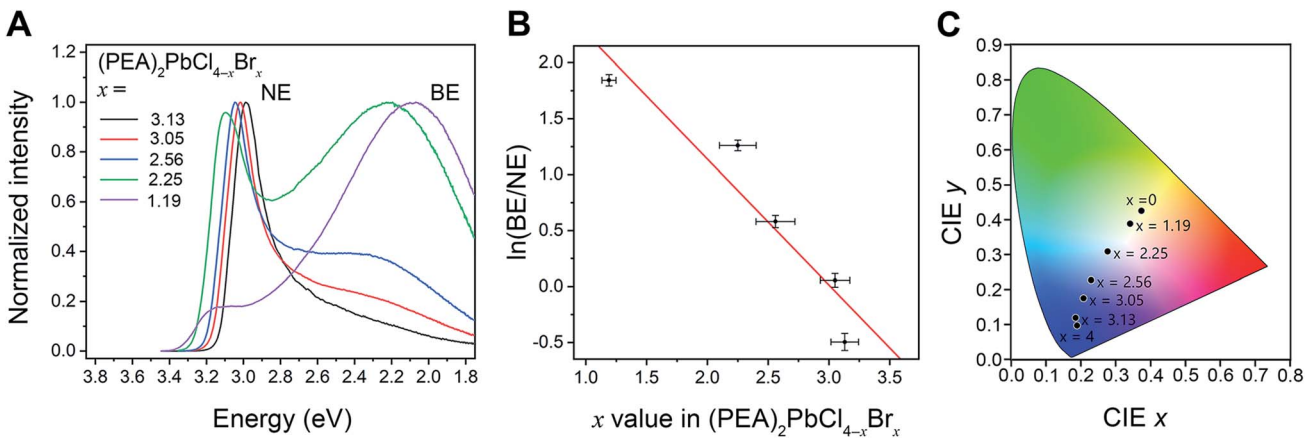

Fig. 3 (A) Room-temperature PL of the (001) perovskite $(PEA)_2PbCl_{4-x}Br_x$ as a function of x featuring the broad emission (BE) and the narrow emission (NE), (B) the correlation between ln(BE/NE) and the bromide content (x), and (C) the corresponding chromaticity coordinates of the emission. The PL data in (A) are normalized to the most intense emission feature for each material.

of the BE peak relative to the intensity of the NE and the energy of the E_{max} of the NE and BE slightly redshift and blueshift, respectively. The endmember (BDA)$PbBr_4$ retains some BE consistent with the relatively high D_{out} value of 20.7°.[3j] Plotting the chromaticity coordinates of (BDA)$PbCl_{4-x}Br_x$, we again observe that the emission color can be continuously tuned from cold white to warm white by altering the halide ratio (Fig. S27 and Table S8†).

The emission color of (IEA)$PbCl_{4-x}Br_x$ can similarly be tuned through variation of the halide ratio (Fig. S26–S27 and Table S8†) although the energy of the BE appears relatively invariant as x is increased. The range of E_{max} values for the BE in (IEA)$PbCl_{4-x}Br_x$ is 30 meV, an order of magnitude smaller than the 400 meV shift observed in $(PEA)_2PbCl_{4-x}Br_x$. The position of the NE peak redshifts with increasing x as observed in the other mixed-halide perovskites. Although the variation in emission is comparatively less smooth in the (IEA)$PbCl_{4-x}Br_x$ series, when the chromaticity coordinates from each perovskite are plotted it is clear that the emission color can still be tuned from cold white to warm white using the halide ratio (Fig. S27 and Table S8†). We note the x values for (BDA)$PbCl_{4-x}Br_x$ and (IEA)$PbCl_{4-x}Br_x$ were estimated from concentrations in solution and are likely less accurate than the values for the other perovskite families studied here.

We have shown for three different families of (001) mixed halide perovskites $A_2PbCl_{4-x}Br_x$ (A^+ = PEA) and $APbCl_{4-x}Br_x$ (A^{2+} = BDA, IEA) that we can tune the halide ratio to afford white-light emission at room temperature. Data for two more perovskite families are presented in Sections 2.3.2 and 2.3.3. Thus the generality of the broad yellow emission in (001) Pb–Cl perovskites we describe, taken together with the behavior of the mixed-halide perovskites presented here and elsewhere[18] suggest that any (001) perovskite can be tuned to emit white light at room temperature simply by altering the ratio of halides used in the crystallization solution.

2.3.2. Halide composition and octahedral tilts. Our prior studies on the temperature-dependent PL of nine representative perovskites suggested that all (001) Pb–Br perovskites have both FE and STE states, which can produce the NE and the BE, respectively. Thus the difference in activation energies (E_a) for exciton detrapping from the STE state and trapping from the FE state dictates whether the narrow or the broad emission is favored at a given temperature (Fig. 4A).[3j] Here, the difference in E_as of trapping and detrapping is given by the self-trapping depth (ΔG_{STE}). The ratio of NE to BE intensities is related to ΔG_{STE}:

$$\ln\frac{BE}{NE} \propto \ln\frac{k_{r,s}}{k_{r,f}} - \frac{\Delta G_{STE}}{k_B T}$$

where $k_{r,s}$ and $k_{r,f}$ are the radiative emission rate constants for the STE and FE states, respectively, k_B is Boltzmann's constant, and T is temperature.[3j] In most (001) Pb–Br perovskites, ΔG_{STE} is small and excitons can freely detrap from the STE state to the FE state at room temperature (Fig. 4A). The shorter emission lifetime of the FE state compared to that of the STE state[5] leads to predominant NE. Indeed, the redshift we observe in the BE of mixed-halide perovskites with decreasing Br content is

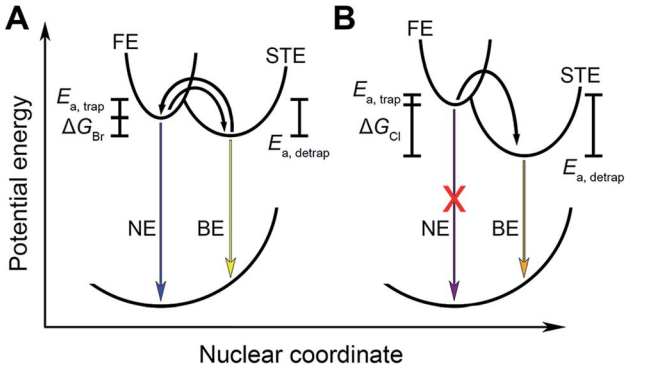

Fig. 4 Energy diagram schematically depicting narrow emission (NE) from the free exciton (FE) and broad emission (BE) from the self-trapped exciton (STE) states of typical (001) (A) Pb–Br and (B) Pb–Cl perovskites. The stabilization of the STE state over the FE state is given by the self-trapping depth: $\Delta G_{STE} = E_{a,\,detrap} - E_{a,\,trap}$ (where $E_{a,\,detrap}$ and $E_{a,\,trap}$ denote activation energies of detrapping out of the STE state and trapping into the STE state, respectively).

consistent with increased stabilization of the STE state. The combination of STE stabilization and the blueshift in FE absorption with increasing Cl content leads to an increased ΔG_{STE} value, which may explain the persistence of the BE for Pb–Cl perovskites.

We previously found that ΔG_{STE} is correlated with the value of the out-of-plane interoctahedral tilt, D_{out}, for (001) Pb–Br perovskites,[3j] where larger values of D_{out} favor the broad emission over the narrow emission. This correlation also holds for the mixed-chloride-bromide perovskites studied here. As described in Section 2.3.1, increasing the Cl content promotes the BE emission over the NE emission, but the specific halide ratio that produces room-temperature white-light emission varies with D_{out}: perovskites with larger values of D_{out} appear to require more bromide-rich compositions, whereas perovskites with smaller D_{out} values appear to require more chloride-rich compositions for white-light emission. To demonstrate this, we synthesized the $(BA)_2PbCl_{4-x}Br_x$ (BA = butylammonium) perovskites as they have small D_{out} values of 2.8° and 0° for the x = 4 and 0 members, respectively.[3i,j] Similar to the other mixed-halide series, the chloride-only x = 0 endmember shows only the BE (Fig. S29 and Table S9†). Intermediate compositions with $1.20 < x < 3.27$ show decreasing intensity of the BE relative to the NE with increasing x, with the bromide-rich x = 3.27 member showing only NE at room temperature (at 3.02 eV, appearing blue).

We compared the emission profiles of $(BA)_2PbCl_{4-x}Br_x$ and $(PEA)_2PbCl_{4-x}Br_x$ perovskites to evaluate the effect of D_{out} on white-light emission. The values of D_{out} for $(PEA)_2PbCl_{4-x}Br_x$ are 10.4° and 6.42° for the x = 4 and x = 0 members, significantly greater than the D_{out} values for the corresponding $(BA)_2PbCl_{4-x}Br_x$ perovskites. The perovskites $(BA)_2PbCl_{2.80}Br_{1.20}$ and $(PEA)_2PbCl_{2.81}Br_{1.19}$ have nearly identical halide composition. However, the PL from $(BA)_2PbCl_{2.80}Br_{1.20}$ is closer to noonday sunlight based on the D65 standard illuminant (chromaticity coordinates of (0.32, 0.36) and a CRI of 89, with a CCT of

6063 K) compared to the PL from $(PEA)_2PbCl_{2.81}Br_{1.19}$. We can interpolate that the ideal halide composition to produce white light with $(PEA)_2PbCl_{4-x}Br_x$ must lie between $x = 1.19$ and $x = 2.25$ (Fig. 3C), which is more bromide-rich than $(BA)_2PbCl_{2.80}Br_{1.20}$. Thus, we find that comparison of perovskites with the PEA and BA cations supports the trend that perovskites with smaller values of D_{out} require more chloride-rich compositions for white-light emission. Since both compositions can be tuned by their halide ratio to emit white light, we further compared the PLQE and stability of the perovskites $(BA)_2PbCl_{2.80}Br_{1.20}$ and $(PEA)_2PbCl_{2.81}Br_{1.19}$ under continuous illumination. We find both $(BA)_2PbCl_{2.81}Br_{1.19}$ and $(PEA)_2PbCl_{2.80}Br_{1.20}$ to have modest and similar PLQEs of 1% and 2%, respectively (Tables S7 and S9†). These are comparable efficiencies to previously reported white-light-emitting perovskite compositions.[18] Both $(BA)_2PbCl_{2.81}Br_{1.19}$ and $(PEA)_2PbCl_{2.80}Br_{1.20}$ do not show any new peaks characteristic of halide segregation under continuous UV illumination even after several hours of illumination (Fig. S30 and Table S10†). In contrast, mixed-bromide-iodide 3D perovskites, such as $(CH_3NH_3)Pb(Br_xI_{1-x})_3$ with $x > 0.2$, show changes in PL energy within a minute of irradiation, attributed to light-induced halide segregation.[19] The drop in overall emission intensity of $(BA)_2PbCl_{2.81}Br_{1.19}$ and $(PEA)_2PbCl_{2.80}Br_{1.20}$ over hours of irradiation is likely due to the instability of the photoexcited state to ambient conditions, although the white-light emission from halide perovskites has been shown to be stable in vacuum for 3 months.[2b]

2.3.3. (110) perovskites. The emission of (110) Pb–Br perovskites can also be tuned with Cl incorporation, similar to the (001) perovskites. The (110) $(BIEA)PbCl_{4-x}Br_x$ perovskites crystallize in the same space group with only minor changes in structure as the halide ratio varies. These perovskites show a modulated structure and the $x = 0$ and 4 members crystallize in the same superspace group with a similar q-vector (Table S3†). Unlike (001) Pb–Br perovskites, the emission of the (110) perovskite $(BIEA)PbBr_4$ is dominated by the BE centered at 2.14 eV. The NE can be observed only as a shoulder at *ca.* 3.09 eV. The spectrum can be fit to extract an estimate for ln(BE/NE) of 1.97. Increasing x still causes a slight redshift in the NE and a blueshift of the BE by 4 and 13 meV, respectively (Fig. S32†). The ln(BE/NE) also decreases with increasing bromide content, but the value is always relatively large and positive. Thus, increasing the Cl content appears to stabilize the STE over the FE state in (110) perovskites as well, though the magnitude of these changes is smaller than that seen in the (001) perovskites because of the similarity of the PL in $x = 0$ and 4 (110) perovskites. Furthermore, (110) Pb–Br perovskites typically show white-light emission at room temperature and therefore adding Cl decreases the emission's color rendition. For example, examining the chromaticity coordinates for $x = 0$, 1.75, 2.17, and 4 in this series (Fig. S33 and Table S11†), the emission from $(BIEA)PbBr_4$ most closely resembles white light with chromaticity coordinates of (0.34, 0.39), a CCT of 5365 K, and CRI of 81. Thus, for a Pb–Br perovskite that begins with a warm white emission, increasing the Cl content will only shift the emission color further from pure white.

3. Conclusion

By studying ten different 2D Pb–Cl perovskites, we find that all the materials show a broad PL at room temperature, suggesting that, in contrast to Pb–Br perovskites, broad emission is common to all 2D Pb–Cl perovskites. Our optical data suggest that Cl incorporation stabilizes the self-trapped excitonic state, favouring the broad emission over the narrow, free excitonic emission. The emission is strikingly similar across all Pb–Cl perovskites studied and we find no correlation between the broad emission and various structural parameters in the inorganic sheets, in contrast to prior reports on Pb–Br perovskites. While the emission from the (001) Pb–Cl chloride perovskites is broad, the PL does not approximate white light well, typically appearing yellow-orange. However, by alloying Br to the halide site, white light can be reliably obtained from mixed chloride-bromide perovskites. Importantly, synthesizing mixed-bromide-chloride perovskites appears to be a simple and universal strategy for obtaining white light at room temperature from layered lead-halide perovskites.

Conflicts of interest

There are no conflicts to declare.

Author contributions

E. J. C. and A. C. S. performed the syntheses and all characterization with guidance from H. I. K. The manuscript was written with contributions from all authors.

Acknowledgements

This work was supported by the National Science Foundation (DMR-1904443). A. C. S. was supported by the John Stauffer Stanford Graduate Fellowship. SCXRD studies were performed at the Stanford Nano Shared Facilities (SNSF), supported by the National Science Foundation under award ECCS-2026822.

Notes and references

1 M. D. Smith, B. A. Connor and H. I. Karunadasa, *Chem. Rev.*, 2019, **119**, 3104–3139.
2 (*a*) E. R. Dohner, E. T. Hoke and H. I. Karunadasa, *J. Am. Chem. Soc.*, 2014, **136**, 1718–1721; (*b*) E. R. Dohner, A. Jaffe, L. R. Bradshaw and H. I. Karunadasa, *J. Am. Chem. Soc.*, 2014, **136**, 13154–13157.
3 (*a*) L. Mao, P. Guo, M. Kepenekian, I. Hadar, C. Katan, J. Even, R. D. Schaller, C. C. Stoumpos and M. G. Kanatzidis, *J. Am. Chem. Soc.*, 2018, **140**, 13078–13088; (*b*) Z. Wu, C. Ji, Z. Sun, S. Wang, S. Zhao, W. Zhang, L. Li and J. Luo, *J. Mater. Chem. C*, 2018, **6**, 1171–1175; (*c*) X. Li, P. Guo, M. Kepenekian, I. Hadar, C. Katan, J. Even, C. C. Stoumpos, R. D. Schaller and M. G. Kanatzidis, *Chem. Mater.*, 2019, **31**, 3582–3590; (*d*) B. Febriansyah, D. Giovanni, S. Ramesh, T. M. Koh, Y. Li, T. C. Sum, N. Mathews and J. England, *J. Mater. Chem. C*, 2020, **8**,

889–893; (*e*) C. Lermer, S. P. Harm, S. T. Birkhold, J. A. Jaser, C. M. Kutz, P. Mayer, L. Schmidt-Mende and B. V. Lotsch, *Z. Anorg. Allg. Chem.*, 2016, **642**, 1369–1376; (*f*) L. Mao, Y. Wu, C. C. Stoumpos, B. Traore, C. Katan, J. Even, M. R. Wasielewski and M. G. Kanatzidis, *J. Am. Chem. Soc.*, 2017, **139**, 11956–11963; (*g*) K. Thirumal, W. K. Chong, W. Xie, R. Ganguly, S. K. Muduli, M. Sherburne, M. Asta, S. Mhaisalkar, T. C. Sum, H. S. Soo and N. Mathews, *Chem. Mater.*, 2017, **29**, 3947–3953; (*h*) S. Wang, Y. Yao, Z. Wu, Y. Peng, L. Li and J. Luo, *J. Mater. Chem. C*, 2018, **6**, 12267–12272; (*i*) C. Ji, S. Wang, L. Li, Z. Sun, M. Hong and J. Luo, *Adv. Funct. Mater.*, 2019, **29**, 1805038; (*j*) M. D. Smith, A. Jaffe, E. R. Dohner, A. M. Lindenberg and H. I. Karunadasa, *Chem. Sci.*, 2017, **8**, 4497–4504.

4 (*a*) M. P. U. Haris, R. Bakthavatsalam, S. Shaikh, B. P. Kore, D. Moghe, R. G. Gonnade, D. D. Sarma, D. Kabra and J. Kundu, *Inorg. Chem.*, 2018, **57**, 13443–13452; (*b*) R. Gautier, F. Massuyeau, G. Galnon and M. Paris, *Adv. Mater.*, 2019, **31**, e1807383; (*c*) H. Lin, C. Zhou, Y. Tian, T. Besara, J. Neu, T. Siegrist, Y. Zhou, J. Bullock, K. S. Schanze, W. Ming, M.-H. Du and B. Ma, *Chem. Sci.*, 2017, **8**, 8400–8404.

5 T. Hu, M. D. Smith, E. R. Dohner, M. J. Sher, X. Wu, M. T. Trinh, A. Fisher, J. Corbett, X. Y. Zhu, H. I. Karunadasa and A. M. Lindenberg, *J. Phys. Chem. Lett.*, 2016, **7**, 2258–2263.

6 R. T. Williams and K. S. Song, *J. Phys. Chem. Solids*, 1990, **51**, 679–716.

7 D. Cortecchia, J. Yin, A. Bruno, S.-Z. A. Lo, G. G. Gurzadyan, S. Mhaisalkar, J.-L. Brédas and C. Soci, *J. Mater. Chem. C*, 2017, **5**, 2771–2780.

8 J. E. Thomaz, K. P. Lindquist, H. I. Karunadasa and M. D. Fayer, *J. Am. Chem. Soc.*, 2020, **142**, 16622–16631.

9 (*a*) T. Ishihara, in *Optical Properties of Low–Dimensional Materials*, DOI: **10.1142/9789814261388_0006**, pp. 288–339; (*b*) K. Tanaka, T. Takahashi, T. Kondo, K. Umeda, K. Ema, T. Umebayashi, K. Asai, K. Uchida and N. Miura, *Jpn. J. Appl. Phys.*, 2005, **44**, 5923–5932; (*c*) K. Pradeesh, K. N. Rao and G. V. Prakash, *J. Appl. Phys.*, 2013, **113**, 083523; (*d*) N. Kawano, M. Koshimizu, Y. Sun, N. Yahaba, Y. Fujimoto, T. Yanagida and K. Asai, *J. Phys. Chem. C*, 2014, **118**, 9101–9106.

10 (*a*) Y. Li, G. Zheng and J. Lin, *Eur. J. Inorg. Chem.*, 2008, **2008**, 1689–1692; (*b*) Y. Y. Li, C. K. Lin, G. L. Zheng, Z. Y. Cheng, H. You, W. D. Wang and J. Lin, *Chem. Mater.*, 2006, **18**, 3463–3469; (*c*) Y. Y. Guo, L. J. Yang, S. Biberger, J. A. McNulty, T. Li, K. Schotz, F. Panzer and P. Lightfoot, *Inorg. Chem.*, 2020, **59**, 12858–12866.

11 (*a*) D. G. Billing and A. Lemmerer, *CrystEngComm*, 2009, **11**, 1549–1562; (*b*) M. Braun and W. Frey, *Z. Kristallogr. – New Cryst. Struct.*, 1999, **214**, 335; (*c*) M. Braun and W. Frey, *Z. Kristallogr. – New Cryst. Struct.*, 1999, **214**, 337; (*d*) M. Braun and W. Frey, *Z. Kristallogr. – New Cryst. Struct.*, 1999, **214**, 331; (*e*) M. Braun and W. Frey, *Z. Kristallogr. – New Cryst. Struct.*, 1999, **214**, 333; (*f*) A. B. Corradi, A. M. Ferrari, G. C. Pellacani, A. Saccani, F. Sandrolini and P. Sgarabotto, *Inorg. Chem.*, 1999, **38**, 716–721; (*g*) C. Courseille, N. B. Chanh, T. Maris, A. Daoud, Y. Abid and M. Laguerre, *Phys. Status Solidi A*, 1994, **143**, 203–214; (*h*) L. Dobrzycki and K. Woźniak, *CrystEngComm*, 2008, **10**, 577–589; (*i*) C. Lermer, S. T. Birkhold, I. L. Moudrakovski, P. Mayer, L. M. Schoop, L. Schmidt-Mende and B. V. Lotsch, *Chem. Mater.*, 2016, **28**, 6560–6566; (*j*) A. Meresse and A. Daoud, *Acta Crystallogr., Sect. C: Cryst. Struct. Commun.*, 1989, **45**, 194–196; (*k*) D. B. Mitzi, *J. Solid State Chem.*, 1999, **145**, 694–704; (*l*) G. A. Mousdis, G. C. Papavassiliou, C. P. Raptopoulou and A. Terzis, *J. Mater. Chem.*, 2000, **10**, 515–518; (*m*) G. C. Papavassiliou, G. A. Mousdis, C. P. Raptopoulou and A. Terzis, *J. Mater. Chem.*, 2000, **55**, 536; (*n*) M. K. Rayner and D. G. Billing, *Acta Crystallogr., Sect. E: Struct. Rep. Online*, 2010, **66**, m659; (*o*) M. Geselle and H. Fuess, *Z. Kristallogr. – New Cryst. Struct.*, 1997, **212**, 241–242.

12 A. B. Corradi, A. M. Ferrari, L. Righi and P. Sgarabotto, *Inorg. Chem.*, 2001, **40**, 218–223.

13 N. Ohta and A. R. Robertson, in *Colorimetry*, DOI: **10.1002/0470094745.ch3**, pp. 63–114.

14 M. W. Lufaso and P. M. Woodward, *Acta Crystallogr., Sect. B: Struct. Sci.*, 2004, **60**, 10–20.

15 K. Robinson, G. V. Gibbs and P. H. Ribbe, *Science*, 1971, **172**, 567–570.

16 (*a*) D. Cortecchia, S. Neutzner, A. R. Srimath Kandada, E. Mosconi, D. Meggiolaro, F. De Angelis, C. Soci and A. Petrozza, *J. Am. Chem. Soc.*, 2017, **139**, 39–42; (*b*) S. Elleuch, A. Lusson, S. Pillet, K. Boukheddaden and Y. Abid, *ACS Photonics*, 2020, **7**, 1178–1187; (*c*) B. Febriansyah, T. Borzda, D. Cortecchia, S. Neutzner, G. Folpini, T. M. Koh, Y. Li, N. Mathews, A. Petrozza and J. England, *Angew. Chem., Int. Ed.*, 2020, **59**, 10791–10796; (*d*) L. Mao, Y. Wu, C. C. Stoumpos, M. R. Wasielewski and M. G. Kanatzidis, *J. Am. Chem. Soc.*, 2017, **139**, 5210–5215.

17 J. Mooney and P. Kambhampati, *J. Phys. Chem. Lett.*, 2013, **4**, 3316–3318.

18 M. D. Smith and H. I. Karunadasa, *Acc. Chem. Res.*, 2018, **51**, 619–627.

19 E. T. Hoke, D. J. Slotcavage, E. R. Dohner, A. R. Bowring, H. I. Karunadasa and M. D. McGehee, *Chem. Sci.*, 2015, **6**, 613–617.